Supplementary Information

We explain the anomalous height increase of the Coulomb blockade peaks under THz irradiation by introducing non-equilibrium effects in the CNT-Dot, in addition to the standard PASET approach[1,2]. The non-equilibrium electron distribution function $g_n(\varepsilon_k)$ for electrons in the dot is computed from solutions of the quantum kinetic equation[3]

$$\frac{\partial g_n(\varepsilon_k)}{\partial t} = I_T(g_n,\varepsilon_k) + I_{\text{ep}}(g_n,\varepsilon_k) \equiv 0 \tag{1}$$

The non-equilibrium PASET term is

$$I_T(g_n,\varepsilon_k) = \sum_m J_m^2(\alpha_{\text{S,D}}) \left\{ \left[\varpi_{k,+}^{\text{S}}(n,m) - \varpi_{k,-}^{\text{S}}(n,m)\right] - \left[\varpi_{k,+}^{\text{D}}(n,m) - \varpi_{k,-}^{\text{D}}(n,m)\right] \right\} \tag{2}$$

where J_m is the modified Bessel function of order m, $\alpha_{\text{S,D}} = e\tilde{V}_{\text{S,D}}/hf$, $\tilde{V}_{\text{S,D}}$ is the THz field induced a.c. voltage on the S(D) barriers and f is the THz field frequency. The source and drain tunneling rates are given by

$$\begin{aligned} \varpi_{k,+}^{\text{S(D)}}(n,m) &= \Gamma_{\text{S(D)}}(\varepsilon_+^{S(D),m})\text{f}(\varepsilon_+^{S(D),m}, T_{\text{bath}})\left[1 - g_n(\varepsilon_k)\right] \\ \varpi_{k,-}^{\text{S(D)}}(n,m) &= \Gamma_{\text{S(D)}}(\varepsilon_-^{S(D),m})\left[1 - \text{f}(\varepsilon_-^{S(D),m}, T_{\text{bath}})\right] g_n(\varepsilon_k)\,. \end{aligned} \tag{3}$$

Here we introduced the electron energies $\varepsilon_{+(-)}^{S(D)} = \varepsilon_k + \Delta E \cdot l + E_{\text{G}} + \Delta U_{n(n-1)}^{\text{S(D)}} + mhf$, where ε_k is the continuous electron energy variable, ΔE is the energy level spacing, l is the level index, m is the number of photons assisting the tunneling process, $\text{f}(\varepsilon_\pm^{S(D),m}, T_{\text{bath}})$ is the Fermi distribution function, and T_{bath} is the temperature of S and D electrodes. The shift $E_{\text{G}} = \alpha_G V_{\text{G}}$ of the electron electrochemical potential in the dot is induced by the gate voltage V_{G}, α_G being the gate efficiency. The changes of electron energy $\Delta U_n^{\text{S}} = \delta(n+1/2) - \eta e V_{\text{SD}}$ and $\Delta U_n^{\text{D}} = \delta(n+1/2) + (1-\eta)\, eV_{\text{SD}}$ correspond to the Coulomb energy δ and to the applied source-drain bias (V_{SD}). Here η is the barrier asymmetry coefficient of the CNT-Dot. An electron tunneling from the source electrode to CNT-Dot will increase the energy of the dot by the Coulomb energy $\delta \simeq e^2/C_{tot} + \Delta E$, where C_{tot} is the total dot capacitance. This tunneling changes the number n of electrons inside the dot, causing the shift of electron energy from $\varepsilon_-^{S(D)}$ to $\varepsilon_+^{S(D)}$. The second term in (Eq. 1) is the electron-phonon collision integral, which in its simplest form can be approximated as

$$I_{\text{ep}}(g_n,\varepsilon_k) = -\frac{g_n(\varepsilon_k) - g_n^{(0)}(\varepsilon_k)}{\tau_{ep}}. \tag{4}$$

Here $g_n^{(0)}(\varepsilon_k)$ is the Fermi distribution function which depends on the electrochemical potential μ in the dot and effective electron temperature T^* which must be determined self-consistently as explained below. Typical electron-phonon relaxation time[4] is $\tau_{ep} \simeq 10^{-12}$ s at $T = 4.2$ K.

The probability that there are n electrons in the CNT-Dot is obtained from the modified master equation that includes the non-equilibrium function $g_n(\varepsilon_k)$. Previous calculations[1,2] assumed the CNT-Dot to be in equilibrium with the lattice.

The electron distribution function $g_n(\varepsilon_k)$ obtained as a solution of the quantum kinetic equation (Eq. 1) is plotted in Figure 6. The red curve represents the "dark current" case (no THz radiation) and corresponds to an effective electron temperature of $T^* = 9.3$ K. Curves 2 and 3 in the same figure correspond to THz frequencies $hf_2 = 0.8\Delta E$ and $hf_3 = 1.2\Delta E$, respectively. Cooling of the CNT-Dot occurs because the "hottest" electrons are extracted faster from the dot when the THz field is applied. The cartoon shown in Figure 5b illustrates the non-equilibrium cooling mechanism of the CNT-Dot. When the THz field is off, an electron injected from source to dot causes the energy level shift $E_0 \rightarrow E_{1_0}$ by $\delta + \Delta E$ (at zero bias) from "0" to "1_0" (see Fig. 5b). When the THz field is on, the absorption/emission of a photon modifies the energy change, e.g., $\delta + \Delta E \rightarrow \delta + \Delta E + hf$. If the THz field frequency $hf < \Delta E$, the electrons populate mainly the level 1_0 (blue curve in Figure 6 shows the corresponding non-equilibrium electron distribution function, g_{ε_k}). The function g_{ε_k} is obtained from the quantum kinetic equation.[3] If $hf \geq \Delta E$, the upper 1_+ level is also populated. Because the tunneling rate $\Gamma_D(\varepsilon_k)$ increases sharply at $\varepsilon_k \simeq E_{1_+}$ ($\Gamma_D(E_{1_+}) >> \Gamma_D(E_{1_0})$), electrons in level 1_+ escape much faster to the drain than they did from 1_0 (thicker green arrow in Fig. 5b). The faster removal of "hottest" electrons induced by the THz field causes the effective electron temperature (T^*) of the CNT-Dot to decrease.

The effective temperatures of the electrons on the dot were derived using a power balance condition $W_T + W_{\rm ep} \equiv 0$ which is satisfied automatically for solution $g_n(\varepsilon_k)$ of the quantum kinetic equation (Eq. 1). Here the power supplied by the PASET tunneling is $W_T = \sum_k \varepsilon_k I_T\{g_n, \varepsilon_k\}$ while the power dissipated due to the inelastic electron-phonon collisions is $W_{\rm ep} = \sum_k \varepsilon_k I_{\rm ep}\{g_n, \varepsilon_k\}$. We also use the condition $n = \sum_k g_n(\varepsilon_k)$, where n is the number of electrons on the CNT-Dot, either with or without the THz radiation.[2] First, we compute n and W_T using the solution $g_n(\varepsilon_k)$ of equation (Eq. 1). Then, we substitute the computed values of n and W_T into the two equations $W_T = \sum_k \varepsilon_k I_T \left\{ g_n^{(0)}(\varepsilon_k, T^*) \right\}$ and $n = \sum_k g_n^{(0)}(\varepsilon_k, T^*)$ which are solved now with respect to T^* and μ for the non-equilibrium case, using $g_n^{(0)}(\varepsilon_k, T^*) = 1/(\exp((\varepsilon_k - \mu)/T^*) + 1)$. Then, we obtain the effective electron temperature T^* and the electrochemical potential μ for the "dark current" case (the THz is off) and for the case when the THz field is on. The above equations have been solved numerically by using the charging energy $\delta = 13.7$ meV, the level spacing $\Delta E = 3.3$ meV, the tunneling rate parameters $\Gamma_S(E_{1_+}) = 0.45$ meV, $\Gamma_D(E_{1_+}) = 0.3$ meV, $\Gamma_D(E_{1_0}) = 0.15$ meV, and the a.c. field amplitude $\tilde{V}_{SD} = 0.8 \times hf/e$. We find that increasing the THz frequency (or amplitude) cools the CNT-Dot and results in the anomalous increase in amplitude of the coulomb blockade peaks (curves 2 and 3 in Fig. 6 correspond to $T^* = 6.9$ and 4.2 K, respectively) observed in our experiment.

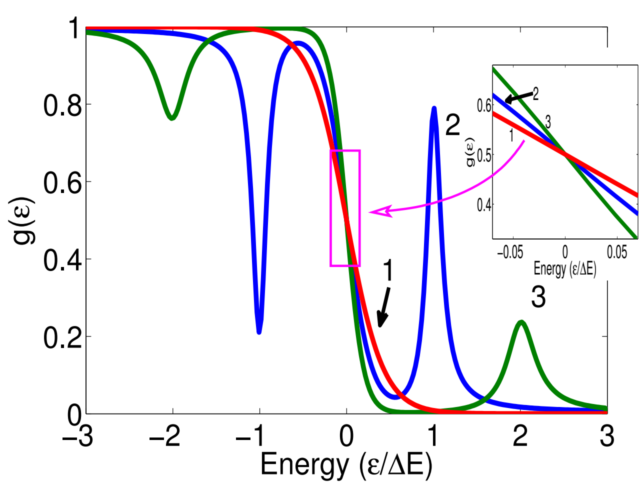

Figure 6 | The distribution function of electrons on the dot: Curve 1 corresponds to the "dark current" while curves 2 and 3 correspond to the THz field on: Curve 2 for $hf_2 = 0.8\Delta E$ and curve 3 for $hf_3 = 1.2\Delta E$. The inset illustrates the increase of tilting the distribution function as the THz field is on and grows: steeper tilting corresponds to the lower effective electron temperature.

[1] Kouwenhoven, L. P., Jauhar, S., Orenstein, J., McEuen, P. L., Nagamune, Y., Motohisa, J. & Sakaki, H. Observation of photon assisted tunneling through a quantum dot. *Phys. Rev. Lett.* **73,** 3443–3446 (1994).

Fuse, T., Kawano, Y., Yamaguchi, T., Aoyagi, Y. & Ishibashi, K. Quantum response of carbon nanotube quantum dots to terahertz wave irradiation. *Nanotechnology* **18,** 044001 (2007).

[2] Averin, D., Korotkov, A. N. & Likharev, K. K. Theory of single-electron charging of quantum wells and dots. *Phys. Rev. B* **44,** 6199–6211 (1991).

[3] Keldysh, L. V. Diagram technique for non-equilibrium processes. *Sov. Phys. JETP* **20,** 1018–1023 (1965).

[4] Park, J.-Y., Rosenblatt, S., Yaish, Y., Sazonova, V., Üstünel, H., Braig, S., Arias, T. A., Brouwer, P. W. & McEuen, P. L. Electron-Phonon scattering in metallic single-walled carbon nanotubes. *Nano Letters* **4,** 517–520 (2004).